Chapter 19
Vibration Energy Harvesting

19.1 A Brief Introduction

There is a long history of development of energy sources with some quite significant moments, such as the discovery of electricity and of nuclear power (both made at the Cavendish laboratory at Cambridge). Other important inventions have been made such as the internal combustion and jet engines. Now with the introduction of electric vehicles it is electricity which is the main transporter of energy from one place to another.

There are two good reasons for studying sources of energy. First, we have the Sustainable Development Goals where goal 7 asks us to "Ensure access to affordable, reliable, sustainable and modern energy for all". Second is the growth in wireless sensors and actuators, the Internet of Things (IoT). We are told to expect the deployment of one trillion IoT devices per year in the near future. These all will need power. Traditionally batteries have been used to power similar devices, but this will be impossible here due to the sheer numbers of IoT devices and the fact that many will be located in remote or harsh environments, such as inside ourselves. Replenishing batteries is not an option.

So, what is a suitable 'modern' energy source, to quote from SDG 7? Well, vibration exists everywhere, car motors and engines, most machinery, ocean waves, the human heart, buildings (which sway in the wind) and so on. This energy exists and is free to harvest, and causes no pollution, except in indirect result of device manufacturing.

In this chapter we shall look at some *approaches* to vibration energy harvesting (VEH) with particular applications such as wave energy, mico-scale energy harvesting, energy from cars and trains and from the wind.

Before we commence, we must make one distinction clear, the difference between *power* and *energy* (and our focus will be on computing powers). We purchase energy in parcels, such as a battery or a litre of fuel. Then we use this up for our radio or car. But we can't buy parcels of energy from our electricity supplier since they provide electricity as a continuous *flow*, and that's what *power* is, it's the flow of electricity along cables just like water flowing down a pipe. Power is measured in *watts*, what does that mean? Take a few examples, a kettle uses about 3,500 watts, a computer perhaps 300 watts, and your brain around 12 watts. That will provide a context for calculations we shall make shortly.

19.2 The nature of VEHs and vibrations

Let's start by considering the nature of vibrations, both natural and man-made. When something vibrates, it keeps on returning to a previous position and its position tends to be bounded on an interval. So our legs swing back and forth and keep returning to the ground position. Such motion almost often has a defined *frequency*; our legs have a frequency of 1 step/second or 1 Hz for walking. A car engine rotating at 3000 rpm rotates at 3000/60 = 50 rev/sec or 50Hz and if there are 4 pistons then we expect an additional vibration of 200 Hz. Some typical frequencies are shown in Table 19.1. Compared with music and speech, all these are quite low.

Table 19.1 Some natural and man-made vibration frequencies

Application Example	Frequency (Hz)
Household equipment	< 100
Buildings	< 100
Human body	2 – 3
Bridges	2 – 3
Freight train	0.5 – 2.0
Ocean waves	0.75

You know that any repetitive signal can be synthesized from a number of sine waves, so the analysis presented below will focus on the sine wave which is the simplest form of vibration. Of course, not all vibrations can so be synthesized, vibrations associated with earthquakes tend to be random in nature, a bit like white noise.

The general VEH system has the structure shown below, and with the exception of the power electronics, we shall need to consider each component which may vary with application. On the left is the vibration source, this usually feeds into some mechanical system which is connected to a transducer which converts mechanical power to electrical power. The dotted rectangle indicates the VEH components.

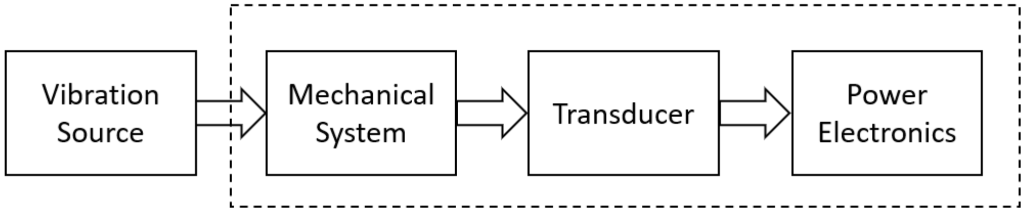

There is one issue which we should consider, and this forms the greatest part of current research into VEHs. Often the vibration source has a *range* of frequencies, as indicated in Table 19.1, but the ideal VEH responds most optimally to a single frequency. We shall see the reason for this in the next section. So much research considers how to *broaden* the response bandwidth, and we shall present some approaches below.

Let's return to electrical power and look at some typical powers which can be harvested from natural and man-made systems, Table 19.2 provides an overview. We shall discuss *piezoelectric*, *electromagnetic*, *electrostatic* and *vortex-induced vibration* transducers in this chapter. One important vibration source is high-rise buildings, especially in earthquake zones. These are made from steel and concrete which do not damp vibrations very well, in fact they are fitted with shock absorbers to absorb vibrations, where the energy is dissipated (wasted) as hear. An estimate of the power which could be harvested from a 75 storey building is about 75,000 watts. That could easily power the entire building. Wave energy has a huge potential, an estimate of the power available from the Gulf of Mexico is about 20,000 Megawatts equivalent to about 20 medium-sized nuclear power stations. At the other end of the spectrum are IoT devices which consume between 0.1 and 1.0 milliwatts of power.

Table 19.1 Typical harvestable powers

Application Example or Device	**Power**
Piezoelectric	10 – 40 μW
Electromagnetic	2.5 – 5.5 W
Electrostatic	1 – 300 μW
Vortex Induced Vibrations (water)	200 W
Vortex Induced Vibrations (wind)	100 W
Car shock absorber	300 W
Train track	200 W
Tuned Mass Damper (buildings)	75 kW
Humans	0.5 W

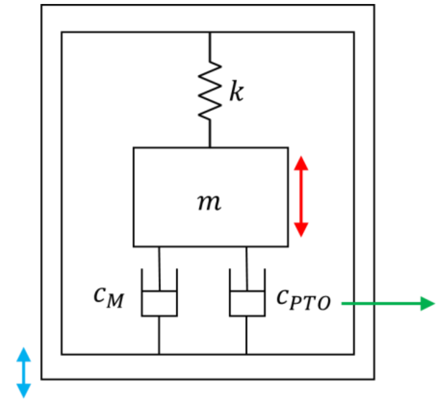

Figure 19.1 Basic structure of a VEH.

19.3 Mechanical Behaviour of a VEH

The structure of a VEH mechanical system is shown in Fig.19.1. The outer frame receives the vibrations (blue arrow) and contains a mass *m* on a spring of stiffness *k*, and the mass responds to the vibrations by oscillating (red arrow). Note the response (red) is larger than the excitation (blue). Underneath the mass we see two 'dashpots' which represent damping (power absorption) of the mass. On the left is c_M which is the *mechanical* damping, due to friction and on the right is c_{PTO} which is damping due to the power take-off device (PTO) or transducer. This is how we get power out of the harvester, shown by the green arrow. Setting the value of c_{PTO} is an important part of the VEH design; you may think that we should have $c_{PTO} > c_M$ to maximize power output since friction is a bad thing, but we shall discover that the maximum power output is achieved when $c_{PTO} = c_M$. Interesting stuff to come.

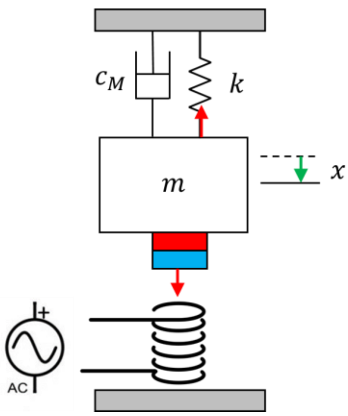

Figure 19.2 A simple oscillator excited by a force.

19.3.1 A Simplified Mechanical System

Before we discuss the mechanical system (Fig.19.1), it is interesting to consider a simpler system shown in Fig.19.2 where we apply a force to excite the motion. A magnet is attached to the bottom of the mass, and an alternating current passed through a coil underneath; this applies a sinewave *force* to the mass. The red arrows show forces (as always), there is a downward force on the magnet, and the spring reacts by pulling upwards, since the mass has moved down, shown by the displacement *x*.

To understand (and simulate) the behaviour of this system, we must build an ordinary differential equation ODE which models the system. This can be coded and solved numerically. To do this, we look at all the forces acting on the mass and use this to calculate its acceleration. Here are the variables we need.

position	x
velocity	$v = \dot{x}$
acceleration	$a = \dot{v} = \ddot{x}$

The dot above the symbols means differentiation with time, so $\dot{x}$ means the rate of change of displacement, which is velocity. So we can enumerate the forces in Fig.19.2.

Origin of force	**Maths expression**
magnet	$F(t) = F_0 \cos(2\pi f t)$
spring	$-kx$
damper	$-c_M \dot{x}$

Let's briefly review these terms. The magnet force is oscillating nicely with frequency *f*. The spring force is proportional to displacement x and acts in the opposite direction. The friction force (damper) is proportional to velocity $\dot{x}$ and acts in the opposite direction, to reduce the velocity, that's what friction does. Now we sum these forces,

$$F = F_0 \cos(2\pi f t) - kx - c_M \dot{x} \qquad (1)$$

and use Newton's 2nd Law $F = ma$ to move towards finding the acceleration,

$$m\ddot{x} = F_0 \cos(2\pi f t) - kx - c_M \dot{x} \qquad (2)$$

To get the acceleration $\ddot{x}$ we divide by the mass m which gives us,

$$\ddot{x} = (F_0/m)\cos(2\pi f t) - (k/m)x - (c_M/m)\dot{x} \quad (3)$$

and finally we make some substitutions so that we end up with a simplified expression

$$\boxed{\ddot{x} = a_0 \cos(\omega t) - \omega_0^2 x - 2\beta\dot{x} \quad (4)}$$

Let's look at the substitutions we have made. We have replaced the term involving frequency $2\pi f$ with the angular frequency ω. While f is in cycles/sec ω is in radians/sec. Whenever you see any ω (with subscripts, perhaps) then think 'frequency. Then we have replaced *(k/m)* with ω_0^2. Aha another omega, so *k/m* has something to do with frequency

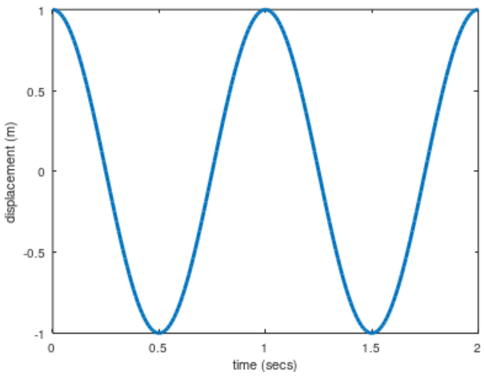

Figure 19.3 Solution of equ. (19.5) for k = 2pi and m=1.

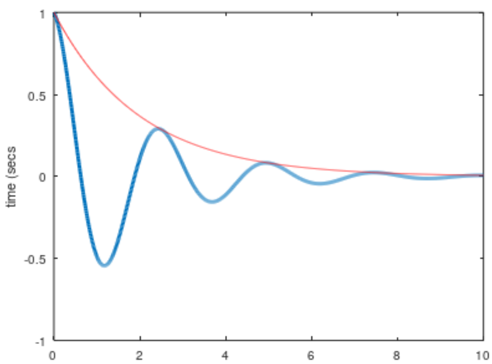

Figure 19.4 Solution of equ. 19.6 with k=2pi, m=1 and beta=0.5.

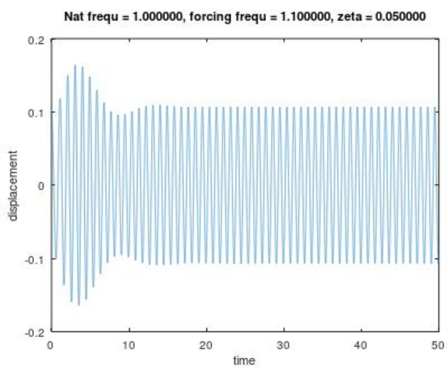

Figure 19.5 Numerical solution to equ. (19.4)

as we soon shall see. Finally, the damping coefficient c_M/m has been replaced by 2β. All these substitutions have been made to make further work more transparent. Let's now look at some solutions to equ (4).

Case 1. Here we set forcing to zero, $a_0 = 0$, and damping to zero, $\beta = 0$. We find that the mass oscillates with frequency ω_0 when we give the mass an initial displacement *A*. The equation for *x* is just,

$$x(t) = A\cos\omega_0 t \qquad (5)$$

and is shown in Fig.19.3. The frequency ω_0 is called the 'natural frequency' of oscillation since it is given by the parameters of the system, k and m.

Case 2. Here we set forcing to zero, $a_0 = 0$ but we have some damping. Again the mass oscillates but its amplitude decreases with time,

$$x(t) = A\,e^{-\beta t}\cos\omega_0 t \qquad (6)$$

and is shown in Fig.19.4. The term $e^{-\beta t}$ produces the decreasing envelope, shown as the red curve, hardly surprising since this involves the damping coefficient β. The greater the damping coefficient, the faster the amplitude decays. To estimate by how much, in time $t = 1/\beta$ the amplitude drops to *1/e* times its starting value which is about *1/3*.

Case 3. Here we look at the *static* behaviour of the mass; there is no acceleration and no velocity and a constant forcing term a_0 with $\omega = 0$. The solution to (19.4) is a constant displacement

$$x = \frac{a_0}{\omega_0^2} \qquad (7)$$

Finally we come to the **general case** solution of (19.4) where there is forcing and also damping. The solution turns out to be,

$$x(t) = A\cos(\omega t + \varphi) + A_{tr}e^{-\beta t}\cos(\omega' t + \varphi') \quad (8)$$

There are two terms here. Note that the second term contains the damping factor $e^{-\beta t}$ which approaches zero as time goes on. So this is a *transient* term. The first term is constant and is normally the response we are interested in. Fig.19.5 shows a typical solution, you can clearly see the initial transient term which mainly disappears after about 20 secs.

19.3.2 The Amplitude Response curve

So far we have been laying down the basic concepts and theory for forced harmonic motion. Here we shall develop some important results which we can apply to any VEH. Usually we are very interested in how the response of the mechanical system (its amplitude *A*) depends on the frequency of excitation, ω. The result is stated below without proof,

$$A(\omega) = \frac{a_0}{\sqrt{(\omega_0^2 - \omega^2)^2 + 4\beta^2\omega^2}} \qquad (9)$$

This curve is sketched below.

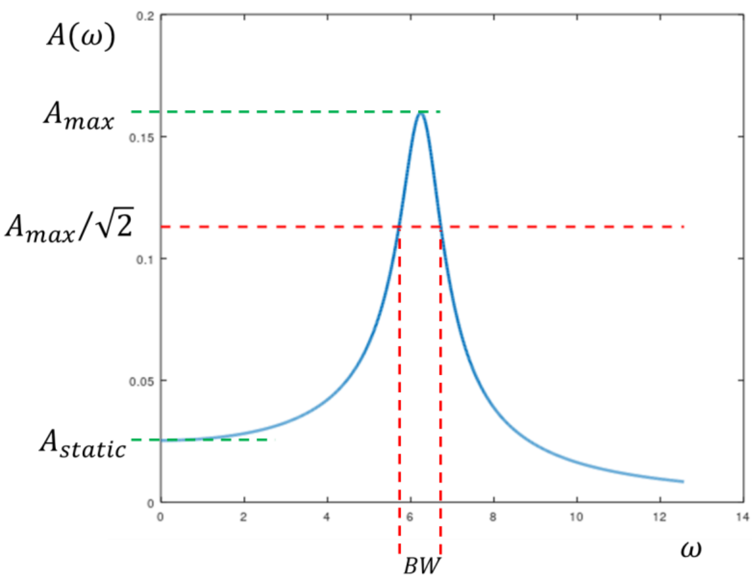

Starting from $\omega = 0$, and increasing ω steadily, the amplitude $A(\omega)$ increases, passes through a maximum, then slowly decreases to zero. It is clear that $A_{max} > A_{static}$ which tells us that this mechanical system has magnified the static displacement. Perhaps the most important takeaway from this plot is that the mechanical system has a maximum response at one particular frequency. The value of this response turns out to be,

$$A_{max} = \frac{a_0}{2\beta\omega_0} \qquad (10)$$

and this tells us something important, the maximum response is greater for small values of damping β. That's our first design guideline. But β enters the story in another way. A dashed line corresponding to $A_{max}/\sqrt{2}$ is shown; this corresponds to a halving of amplitude squared which corresponds to the *power* being halved. The vertical red dashed lines trace this onto the frequency axis where the range of frequencies BW ('bandwidth') is indicated. An approximate expression for the bandwidth turns out to be,

$$BW = 2\beta \qquad (11)$$

Now in designing a VEH we would like it to respond to a large range of frequencies, i.e., have a large bandwidth, and so we need a large β therefore lots of damping. But we have just said that we want a small β to get a large response amplitude. So we have a fundamental limitation for this mechanical system.

> It is not possible to build a mechanical system (as described here) to simultaneously have a very large amplitude response together with a large bandwidth.

As already mentioned, a lot of VEH research is aimed at addressing this problem; some progress is being made, but each improved solution brings with it some undesirables. We can squeeze a little more information out of equ. (10). For systems with a high ω_0, the amplitude is smaller. So lighter objects (smaller mass) tend to vibrate less.

19.4 The Complete VEH Mechanical System

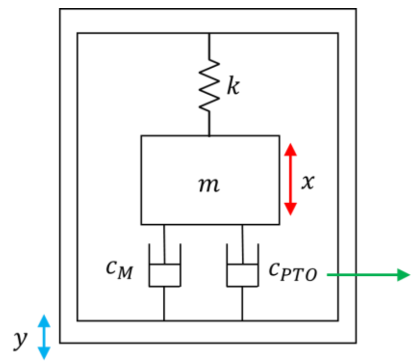

Figure 19.6 WEH mechanical system showing displacement excitation y, of the outer casing.

Let's now return to the complete mechanical system. We'll write down the ODE for this system and then derive an expression for the maximum power which can be extracted by the power-takeoff (PTO) device. Fig. 19.6 reproduces the system we are thinking about. The vibration of the mass is labelled x as usual, but here we indicate that the system is being subject to an external oscillating displacement y rather than a force. If this displacement is $y(t) = y_0 \cos \omega t$ then we must differentiate this twice to get the acceleration which gives us $a(t) = -y_0\omega^2 \cos \omega t$ and we multiply by mass m to get the equivalent force. The ODE, equivalent to eq. (3) can be written down for this case,

$$\ddot{x} = y_0\, \omega^2 \cos(\omega t) - (k/m)x - (c_{Tot}/m)\dot{x} \quad (12)$$

where $c_{Tot} = c_M + c_{PTO}$ is the total damping. Please remember that c_M is the mechanical damping from friction in the machine (we don't like this since it absorbs power) and c_{PTO} is our engineered PTO damping which is what we want, to transduce mechanical power into electrical power. Simplifying this expression, as we did in the previous section leads to this ODE,

$$\boxed{\ddot{x} = y_0\omega^2 \cos(\omega t) - \omega_0^2 x - 2(\beta_M + \beta_{PTO})\dot{x} \quad (13)}$$

Looking back at section 19.3.2 we can immediately write down an expression for the maximum amplitude by replacing a_0 with $y_0\omega_0^2$ and using the two damping coefficients,

$$A_{max} = \frac{y_0\omega_0}{2(\beta_M + \beta_{PTO})} \quad (14)$$

To calculate the maximum output power from the PTO, we multiply c_{PTO} by the velocity of the mass squared. So if the mass is moving according to $x(t) = A \cos \omega t$, then its velocity is $v(t) = -\omega A \sin \omega t$ and the maximum power is, by definition,

$$P_{max} = c_{PTO} v_{max}^2 \qquad (15)$$

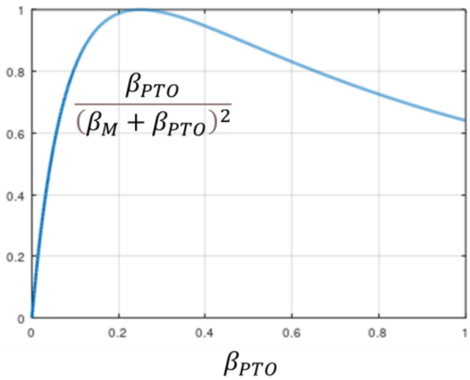

Figure 19.7 Plot of the last factor in 19.26. It's maximum occurs when the PTO damping and the mechanical damping are equal.

Combining eqs. (14) and (15) and performing a little simplification, we have the final expression for the maximum power possible in the PTO device.

$$P_{PTO} = \frac{1}{4} m \omega_0^4 y_0^2 \frac{\beta_{PTO}}{(\beta_M + \beta_{PTO})^2} \qquad (16)$$

This is an extremely useful expression since it allows us to choose the value of β_{PTO}. Keeping everything constant and varying β_{PTO}, when we plot out the last factor in equ. (16) we get the result in Fig. 19.7 where we have set $\beta_M = 0.25$. We see a very interesting result. The factor has a maximum and this maximum occurs when $\beta_{PTO} = 0.25$. In other words the maximum power we can extract occurs when

$$\beta_{PTO} = \beta_M \qquad (17)$$

This is actually a well-know result across science and engineering where maximum power transfer needs to be obtained. You may have come across this if you have built a hi-fi installation, where the impedance of the speakers (e.g. 4 ohms) needs to match the output impedance of the power amplifier (4 ohms).

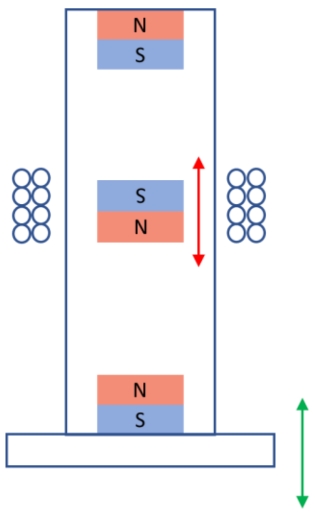

Figure 19.8 Maglev harvester. The central magnet is levitated by repulsion. Circles represent the coil of wire fixed to the frame.

19.5 Magnetic Levitation Harvester

The Maglev harvester is an experimental device which generates electricity when a magnet moves inside a coil of wire. The arrangement is shown in Fig.19.8, where the central magnet is levitated by repulsion from the top and bottom magnets and is constrained so it cannot move horizontally. When the entire device (including the coil) is vibrated (green arrow) then the central magnet lags behind. So there is motion relative to the coil (red arrow) which induces an electric current. The beauty of this device lies in its simplicity, there are no springs, the power takeoff (PTO) is straightforward, and mechanical damping is provided by friction with the cylinder walls, and also air resistance. Using magnets instead of springs introduces some interesting behaviour. Springs are *linear* devices which means they exert a force proportional to extension, but magnets are *non-linear*, you can see this in Fig.19.9. Starting at a displacement of zero and moving to the right, the force increases, but the rate of increase gets larger, in other words the *stiffness* of the spring is increasing. The points in Fig.19.9 are actual measurements, the curve has been fitted and has the form,

$$F(x) = k_1 x + k_2 x^3 \qquad (18)$$

which is a combination of linear and cubic terms. For our device we have $k_1 = 59.7,\ k_2 = 160000$.

Now we know the form of the restoring force, we can write down the ODE for the mechanical part of the maglev harvester,

$$\ddot{x} = -\frac{k_1 x}{m} - \frac{k_2 x^3}{m} - \frac{c}{m}\dot{x} - \frac{\alpha I}{m} - \ddot{y} \qquad (19)$$

Most of these terms should look familiar to you, the second to last includes the generated current I, this is the damping due to the PTO which generates the power we want. The last term represents the acceleration of the device due to the vibrations applied (green arrow in Fig.19.8). In addition, we need an ODE to express the generation of the electric current from the relative motion of coil and central magnet. This is simply,

$$L\dot{I} = -(R_L + R_C)I - \alpha\dot{x} \qquad (20)$$

The terms in this expression are all voltages (you may recognize Ohm's law), the last term is the important one, it tells us that the velocity of the relative motion induces a voltage in the coil. The parameter α which appears in both ODEs expresses the *coupling* between the mechanical system

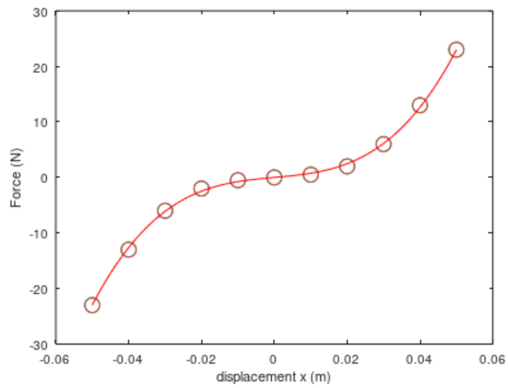

Figure 19.9 Force-displacement curve for the non-linear magnetic 'springs'

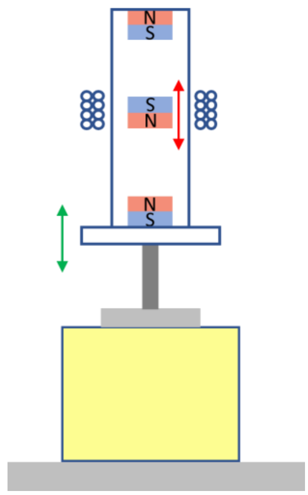

Figure 19.10 Experiment to investigate the maglev VEH showing it mounted on top of a vibration source.

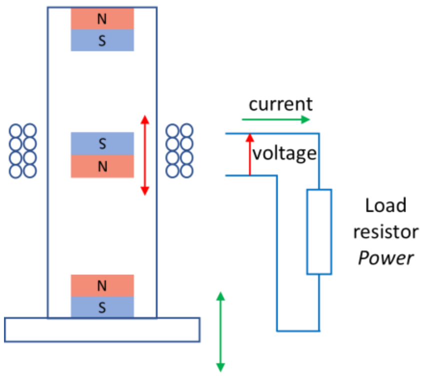

Figure 19.11 Maglev electrical connexions.

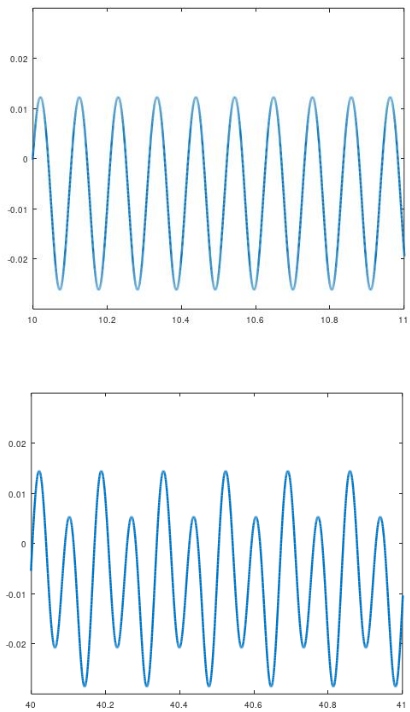

Figure 19.12 Period Doubling. Top omega = 60, bottom omega = 75. Amplitude 0.014.

and the electrical PTO system. R_C is the resistance of the coil and R_L is the resistance of the load (output) resistor.

To investigate the maglev VEH, the experimental arrangement shown in Fig.19.10 is used. The vibrator excites the maglev, the *frequency* of the vibrations is changed, this is the independent variable. The relative displacement of the central magnet and coil is measured as the dependent variable. The current which flows through the load resistor is also measured. The electrical circuit is shown in Fig. 19.11. Typical experimental results are shown below

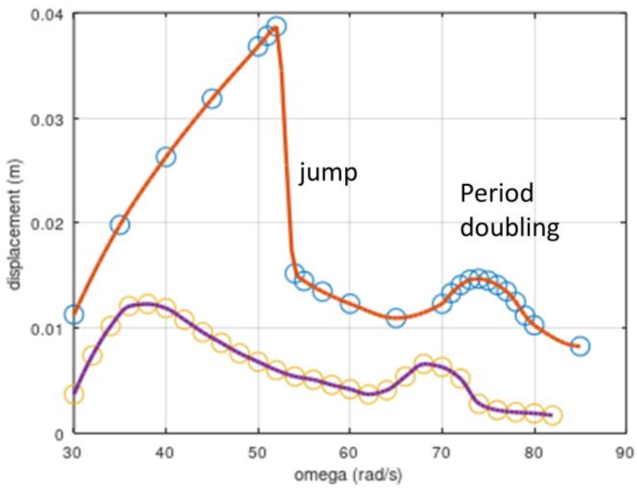

for two driving amplitudes, 0.014 (top) and 0.010 (bottom). Both curves resemble the response curve discussed in section 19.3.2, but there are some differences which can be traced to the *non-linearity* in the magnetic springs. The top curve shows the 'jump phenomenon', when the driving frequency (omega) is increased, the amplitude increases as usual, but just above 50 rad/sec it suddenly jumps down to a low value. Also if you started with a frequency of say 60 rad/sec and slowly decreased it, then the amplitude would jump up to the larger value. The second interesting point is the additional hump between values of 70 and 80 rad/sec. Linear systems do not show this. What is happening here is called 'period doubling'. The magnet-coil relative motion no longer has the same frequency as the applied vibrations, but it has a component at half the frequency. This is shown in Fig. 19.12. Interestingly, the nonlinearity has produced a larger than expected amplitude in this region. Note that the lower amplitude curve does not display the jump phenomenon.

Turning to the actual power produced by the maglev VEH, we need to measure the current produced, this is shown in Fig.19.13 where we see a maximum current of just under 0.05 Amp is produced. The power obtained in a load resistor of 1.2 kOhms is just,

$$P = I^2R = 0.05^2.1200 = 3\,Watts$$

which is actually quite a lot in the realm of VEHs.

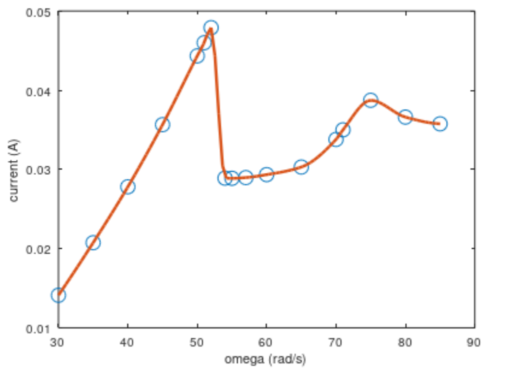

Figure 19.13 Current produced by our maglev as function of omega.

Let's look at the jump phenomenon in more detail and compare the behaviour of a linear system with our nonlinear maglev. The experiment we do is to *sweep* the frequency of the applied vibrations from low to high and then back down to low. The behaviour of both systems is shown below.

Sweep up	Sweep down
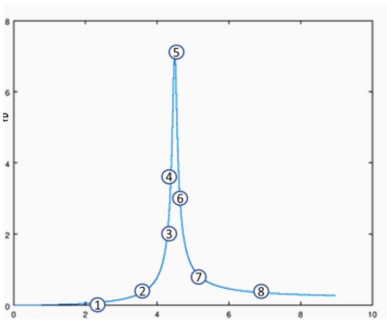	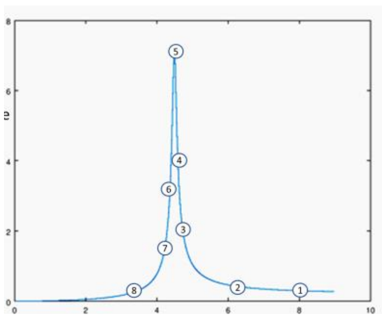
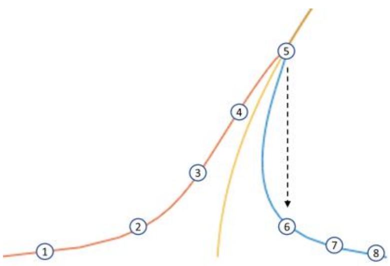	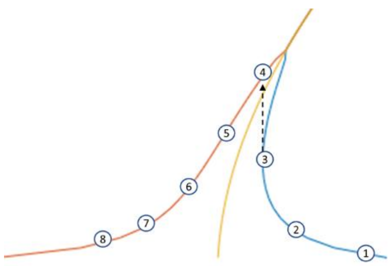

For the linear system (top row) when you sweep up and sweep down, you stay on the curve, but for the non-linear system when you reach point 5 and increase the frequency then you jump down to point 6. On the return journey, at point 3 you suddenly jump up to point 4, also note that the jump up and jump down frequencies are not the same.

19.6 The Piezoelectric VEH

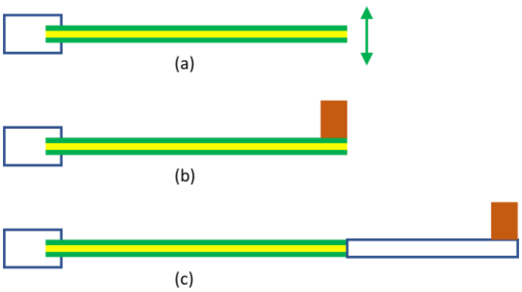

Figure 19.14 Top, single piezo beam, centre with proof mass, bottom with proof mass and plastic beam,

A piezoelectric device is a small, very thin strip which when bent generates a voltage between its surfaces. A typical device has length 30mm, width 5mm and thickness 0.5mm or less. Because of its small size and therefore small mass, the natural frequency of vibration is relatively high, e.g., 300Hz. Many useful vibrations have frequencies well below this and much research is looking at how to lower the natural frequency of a piezo VEH. Two approaches are common, first to attach a 'proof mass' to the end of the device, and second to lengthen the strip using an additional plastic strip. These approaches are the only way to deal with commercial piezoelectric strips, shown schematically in Fig.19.14.

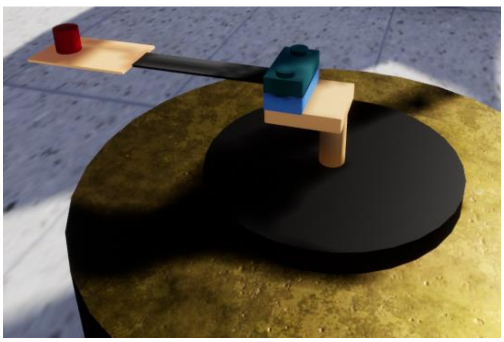

Figure 19.15 Unreal simulation of a piezo VEH

Let's first calculate some frequencies. In general, for a mass-spring we have

$$f = \frac{1}{2\pi}\sqrt{\frac{k}{m}} \qquad (21)$$

where k is the spring stiffness and m is the mass. The stiffness of a cantilever is $k = 2.92EI/l^3$ where l is its length, E is Young's modulus and I the area moment of inertia. The effective mass of a vibrating cantilever is 0.236 times its actual mass. Using these parameters, the mass and stiffness of a device 30mm x 5mm x 0.5mm are 0.19mg and 432 N/m which produces a natural frequency of 218 Hz. Adding a 0.72g proof mass and keeping k the same lowers the natural frequency to 108 Hz. For the third option, a new value for k must be calculated. This lowers the frequency to around 26 Hz. So you can see how some simple modifications allow the operating frequency of the piezo VEH to be designed. A typical experimental arrangement is shown below and a simulation rig in Fig.19.15. This shows an accelerometer

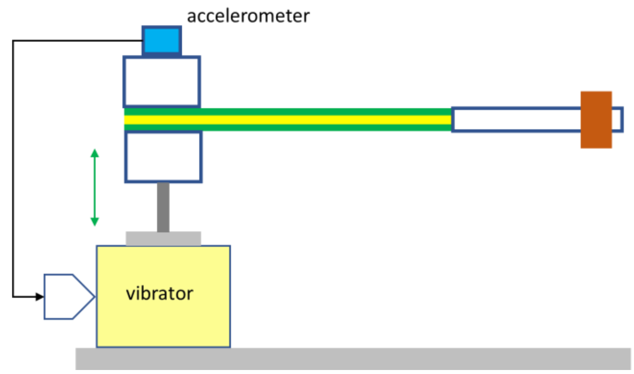

which measures the applied vibration accelerator, it feeds a signal back to the vibrator to keep the acceleration at a constant value even though the frequency of vibration is changed. The ODE for this system is straightforward (and linear!),

$$\ddot{x} = a_0 \cos(2\pi f t) - (k/m)x - (c_M/m)\dot{x} \quad (22)$$

where a_0 is the constant acceleration magnitude. Note, unlike the maglev, there is no additional ODE for the generation of voltage which is proportional to the deflection of the cantilever end. Of course the maximum power is obtained when the load resistor is the same as the resistance of the piezo element.

The response curve for our piezo VEH is shown in Fig.19.16, there are no surprises here which is due to this being a linear system. Typical maximum powers at a constant acceleration of 0.1g are: $4\mu W$ for the single cantilever, $9\mu W$ when the proof mass is added and $12\mu W$ when a composite cantilever with proof mass is used. These are small amounts of power but are small devices indeed.

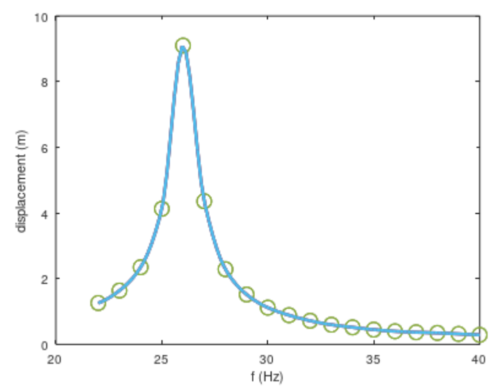

Figure 19.16 Response curve for piezo VEH

We mentioned that one limitation of resonant VEHs is that they work at one specific frequency and researchers are looking at various ways of improving the bandwidth of

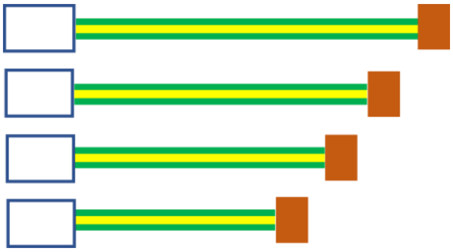

Figure 19.17 Array of piezo elements each with a different frequency.

the VEH while not sacrificing maximum response. Although it can be shown that this is an illusion, it is interesting to consider ways in which this might be done. One way is to construct an array of piezo elements each with a different natural frequency, Fig. 19.17 shows how this can be done by changing the lengths of the piezo elements. Of course, the proof masses could also be varied. The results of simulating an array are shown below. The principal element is tuned to 40 Hz and three additional elements are added, each with a higher frequency. The frequency difference is taken as an independent variable, this difference is the same between adjacent elements. These differences are: 2 Hz (left) 4 Hz

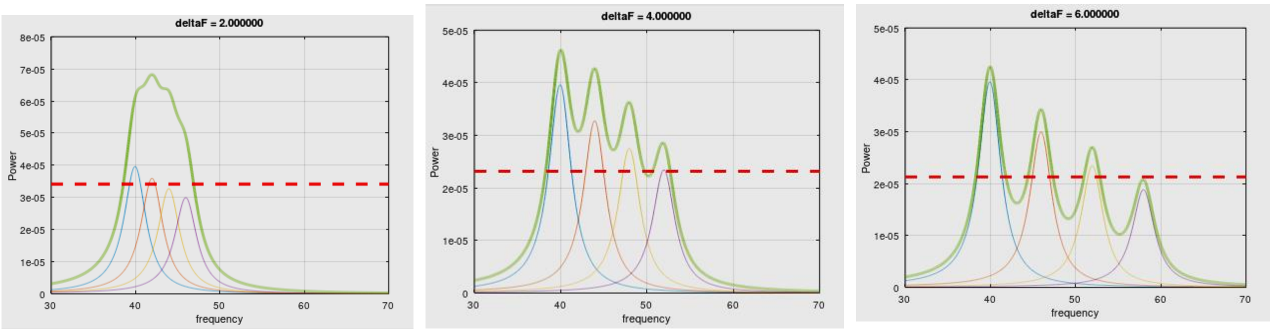

(centre), 6 Hz (right). The red dotted line is drawn at half power which gives us the bandwidth. Clearly, as we increase the frequency difference, the bandwidth increases which is what we want. But the maximum power decreases somewhat. This is easy to understand; first we note that the response of higher-frequency elements gets smaller, this is a consequence of eq. (10) and second, as the frequency difference increases, the individual curves overlap less and less, so there is less summing of power. The half power output of the 40 Hz element is $20\mu W$. If all four elements were tuned to the same frequency, then the half power output would be $80\mu W$ but as the frequency difference increases, the half power falls to $20\mu W$.

Figure 19.18 Cantilever motion restricted by end stop.

A second approach to bandwidth stretching looks a little strange. The vibrating cantilever is restricted by one or more end-stops shown in Fig.19.18. This is modelled as a mass on a spring where the spring constant is much larger than that of the cantilever. The effect of this end stop is quite surprising, it produces a huge increase in the bandwidth of the device (albeit at the expense of lower amplitude). Have a glance at Fig, 19.19 which shows the response of our piezo VEH both with and without the end-stop. The rapid drop in amplitude close to 40 Hz reminds us of the jump-phenomenon for the maglev VEH. Hardly surprising since both involve spring stiffness increasing for larger displacements.

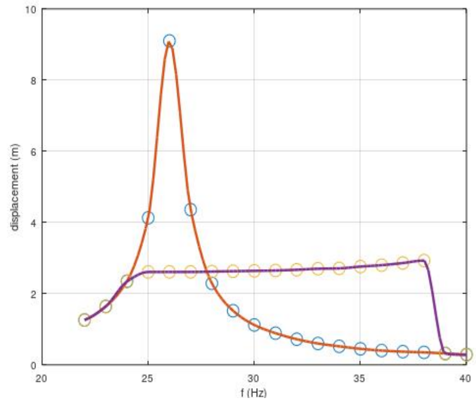

Figure 19.19 Effect of adding an end stop to the piezo cantilever.

19.7 Vortex Induced Vibrations

When a steady flowing fluid (air or liquid) passes around a thin obstacle such as a suspension bridge cable or a tall metal chimney, then the obstacle can start to vibrate. The first observation of this can be traced back to Leonardo Da Vinci who heard Aeolian tones. Up until recently engineers spent most of their efforts in trying to suppress these vibrations which could cause structural damage or collapse, but now they are harnessing the phenomenon, guess what, to make a new generation of VEHs.

To understand vortex induced vibrations (VIV) we need to look at how fluids interact with bodies in their flow, we can do this using computational fluid dynamics (CFD). If we have an airfoil (aeroplane wing) then the fluid flow looks like this. The fluid is coming in from the left (green arrows)

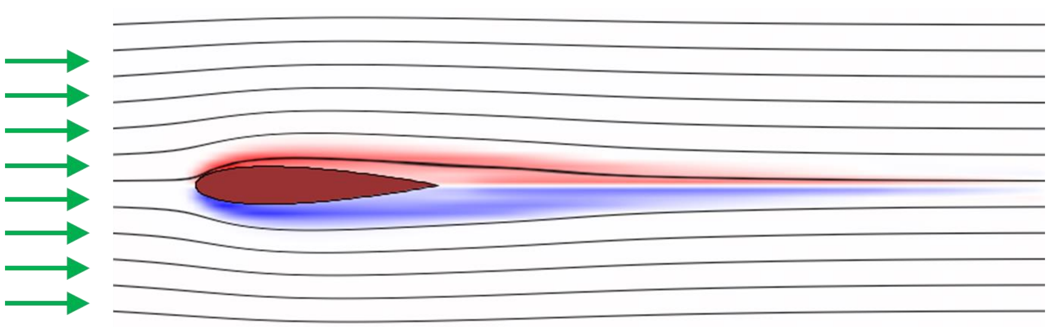

and the black *streamlines* show how the fluid is smoothly passing the airfoil; you've almost certainly seen these on weather maps. Our CFD software tells us about the *rotation* of the fluid as it passes the airfoil. Red is clockwise and blue is anticlockwise. Rotating fluid is called a 'vortex' and the strength of the fluid circulation is called its 'vorticity'. So what happens when a fluid flows past a cylinder? The

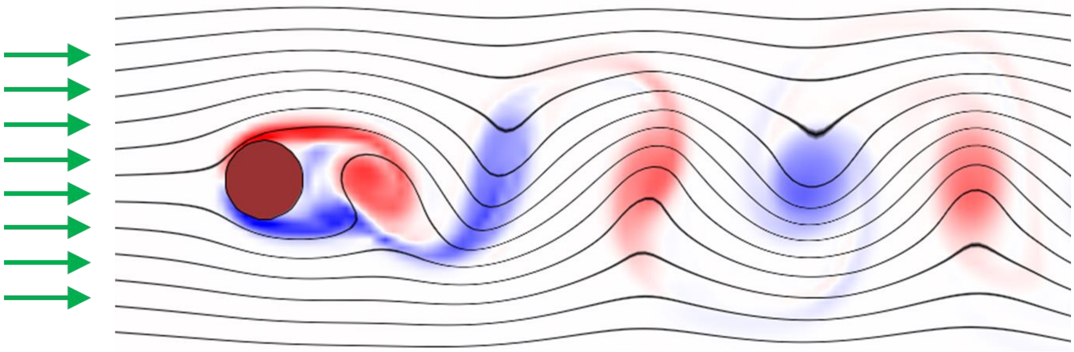

diagram above shows us a surprising consequence. There are two significant differences. First, the streamlines are distorted, fluid seems to be flowing backwards at some points. But the major feature of this flow is that there is a line of vortices behind the cylinder which alternate between clockwise and anticlockwise. These vortices are independent entities, they are *shed* by the cylinder. This line is known as the 'Von Karmen vortex street'. The cylinder is clearly doing quite a lot of work, forcing out all these vortices, and we can apply Newton's third law which tells us that these shed vortices will exert forces onto the cylinder. These forces will cause the cylinder to move, and this movement will ultimately provide us with harvested power.

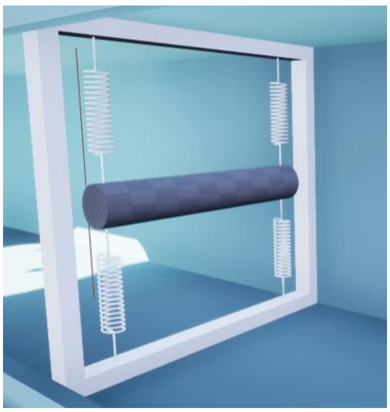

Figure 19.20 Structure of a VIV device. Unreal.

The mechanics of a possible VIV VEH device are shown in Fig.19.20 where the red oscillating cylinder is shown tethered to a frame with four springs. So we have a system which will naturally oscillate with frequency

$$f_0 = \frac{1}{2\pi}\sqrt{\frac{k}{m}} \qquad (23)$$

where k is the stiffness of the springs taken together and m is the mass of the cylinder.

The diagram below shows a moving cylinder above and below the green datum line, the same vertical position for each diagram. Hopefully this will give the impression that the cylinder is moving!

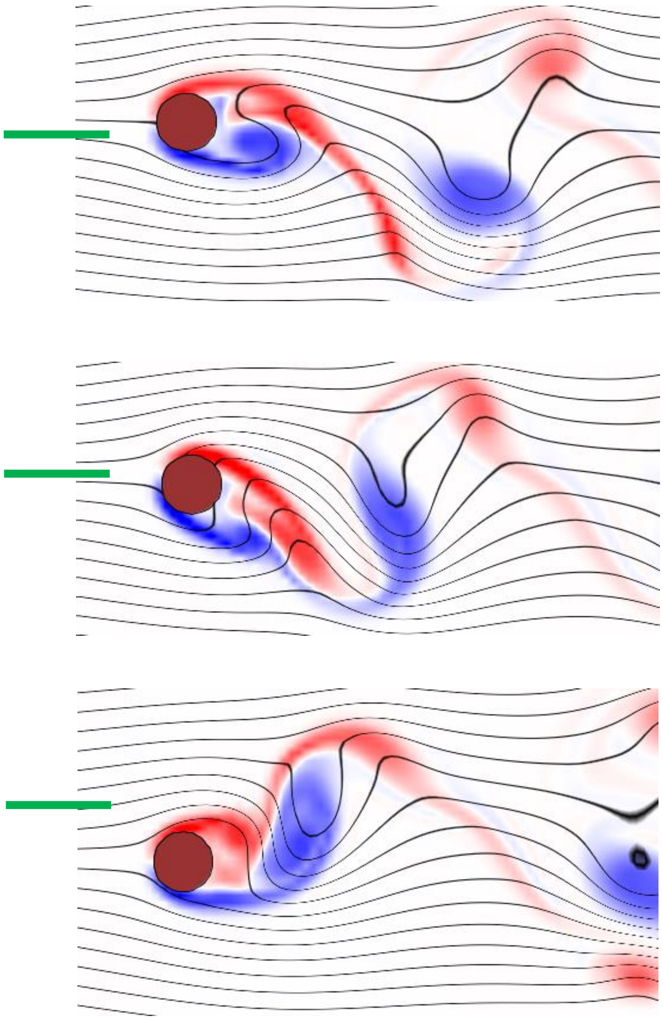

So the cylinder has its own *natural* frequency of oscillation, but there is another frequency involved, the

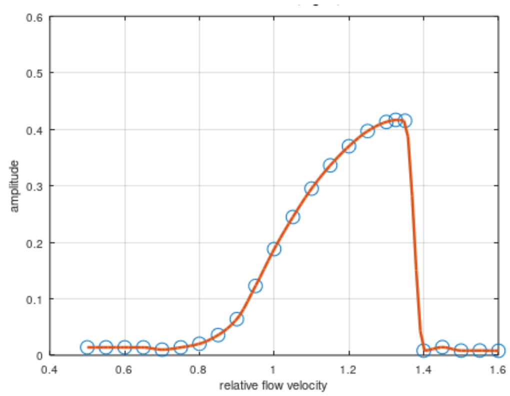

Figure 19.21 Amplitude of oscillation vs. relative flow velocity.

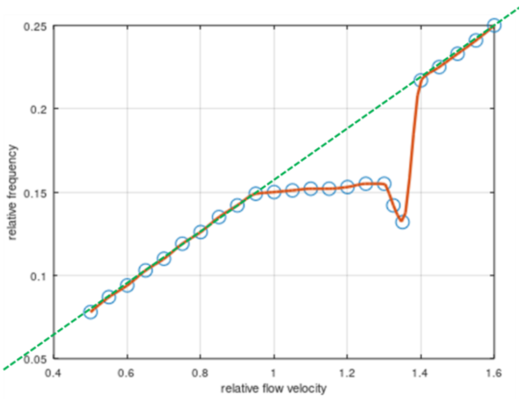

Figure 19.22 Variation of frequency with relative flow velocity showing 'lock-in' phenomenon.

frequency of the vortex shedding. For a *stationary* cylinder, the frequency of vortex production is given by,

$$f_{vortex} = 0.2\frac{U}{d} \qquad (24)$$

where U is the fluid velocity and d the cylinder diameter, finally, a simple expression! When these two frequencies are the same, then we expect to see resonance where the cylinder will oscillate with a maximum amplitude. From equ. (24) we expect to see this at the following fluid velocity,

$$U_R = 5f_0 d \qquad (25)$$

This is confirmed by experiment and simulation as shown in Fig.19.21 where the amplitude is plotted against the fluid velocity divided by U_R.

But there is another phenomenon that emerges. If we plot the observed cylinder oscillation frequency against relative fluid motion, we get the result in Fig.19.22. The green line shows the expected linear increase in cylinder frequency according to equ. (19.34), but in the region of U_R over a range of fluid velocities, the frequency of oscillation is more or less constant at the cylinder's natural frequency given by equ. (19.33). This is called 'lock in' and is extremely interesting since the cylinder is at resonance over a *range* of fluid velocities. Remember the desire to build a VHE with high bandwidth, lock-in is the equivalent for a range of fluid velocities.

It's possible to model the combination of cylinder mass, the springs and a shedding vortex, and to write down ODEs to capture the model. This has been done, and has been used to create the data for Figs. 19.21 and 19.22, though the equations are complicated and will not be discussed here. However the model itself is quite interesting and is shown in Fig.19.23. The cylinder oscillates up and down (green arrow) and the current vortex is attached to the cylinder and oscillates in an arc (blue arrow). So we have a *coupled* oscillator and it turns out that this captures the system dynamics very accurately.

This technology is close to commercialization. The VIVACE system from the University of Michigan has been tested in various rivers and canals and the project is awaiting industrial partners. During research and development, powers of the order of 500-600 W were generated from a single cylinder, the proposed deployment will involve multiple cylinders. A second system which uses VIV from wind is under development, think of a wind turbine without any blades. The device comprises a vertical column fixed at the base with a section free to oscillate, connected to an internal electromagnetic generator similar to the one used in maglev.

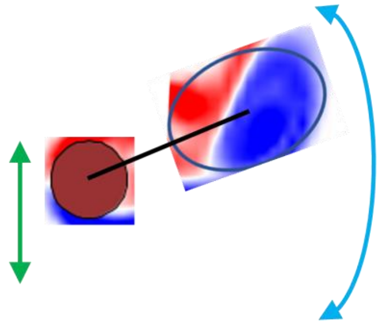

Figure 19.23 Coupled oscillator model of the cylinder spring-mass system and the vortex being shed.

19.8 Microelectromechanical (MEMS) VEH

MEMS devices are tiny silicon-based integrated devices that contain both electronic and mechanical components and can range from micrometres to a few millimetres in size. Applications abound from accelerometers, pressure sensors, hearing aids and microphones to name a few. They are admirably suited to IoT applications since they are fabricated using the same technology used for electronic integrated circuits. They are small enough and can generate enough power for IoT devices.

Fig.19.24 shows the structure of a MEMS VEH. The outer green frame contains stationary comb electrodes (blue) and in the middle there is a proof mass (grey) attached to the red comb electrodes. The mass and red comb can move in a horizontal direction, two vertical springs at the top and bottom provide a restoring force. The device operation is detailed in Fig.19.25, for a single comb electrode overlap. The outer electrodes are given a permanent negative charge so when external vibration makes the left electrode move into the right, then electrons are repelled out of the left electrode and pass through the load resistor generating a voltage and therefore power. The extended spring exerts a force to the left and there is clearly an electrostatic force to the right.

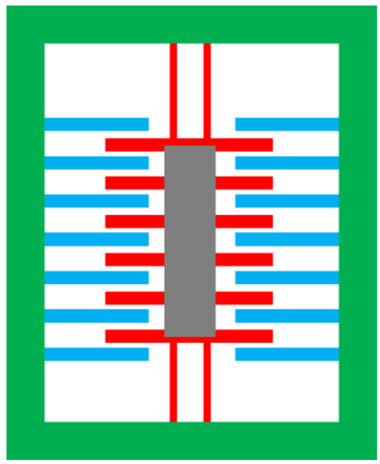

Figure 19.24 Structure of a MEMS VEH showing centre mass (grey) with red and blue comb electrodes.

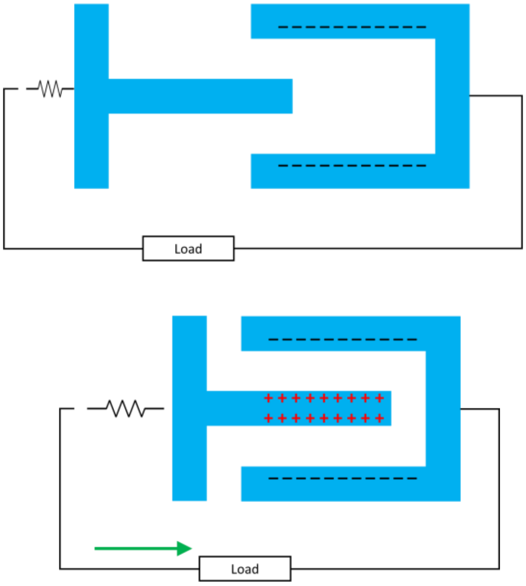

Figure 19.25 Vibration moves the centre electrode into the gap and electrons are repelled from this and pass through the load resistor.

The ODEs for this system are a little complicated, but their structure is understandable. We have an equation for the change of charge on the left and the right comb electrode, and a third equation for the dynamics of the mass.

$$\dot{q}_1 = -\omega_2 \frac{q_1}{1-x} - \omega_{el}(q_1 + q_2) + I_{el}$$

$$\dot{q}_2 = -\omega_2 \frac{q_2}{1+x} - \omega_{el}(q_1 + q_2) + I_{el}$$

$$\ddot{x} = -\frac{\alpha}{2}\left(\frac{q_1}{1-x}\right)^2 + \frac{\alpha}{2}\left(\frac{q_2}{1+x}\right)^2 - x - \beta\dot{x} - a(t) \quad (26)$$

Remember the last equation describes the acceleration of the mass. The first two terms are from the electrostatic forces, then comes -*x* from the spring restoring force, then damping and finally the excitation acceleration.

The above equations were solved to produce a frequency amplitude plot for a device with 500 teeth in the comb, the tooth thickness was 100 μm and the tooth-tooth gap was 6 μm. The load resistance was 70 MΩ and the excitation amplitude was 5 μm. Results are shown below for the amplitude (expressed as a factor of 100 μm) and the power in μW. A maximum power of around 60 μW is obtained.